

A mass spectrometry study of *n*-octane: Electron impact ionization and ion-molecule reactions

C. Q. Jiao

Mobium Enterprises, Inc., 5100 Springfield Pike, Dayton, Ohio 45431-1231

C. A. DeJoseph, Jr. and A. Garscadden^{a)}

Air Force Research Laboratory, Wright-Patterson AFB, Ohio 45433-7251

(Received 27 April 2000; accepted 1 November 2000)

Electron impact ionization of *n*-octane over an energy range of 10–70 eV and the subsequent ion-molecule reactions with the parent molecule have been studied using Fourier-transform mass spectrometry. Molecular ion and fragment ions $C_1^+ - C_6^+$ are produced from the electron impact with a total ionization cross section of $1.4 \pm 0.2 \times 10^{-15} \text{ cm}^2$ between 60 and 70 eV. $C_3H_7^+$ is the most abundant ion at most of the ionizing energies with the exception for $E \leq 16 \text{ eV}$ where $C_6H_{13}^+$ and $C_6H_{12}^+$ are the most abundant. Among the fragment ions only $C_4H_7^+$ and smaller ions react readily with the parent molecule, primarily producing $C_5H_{11}^+$ and $C_4H_9^+$, with rate coefficients of $0.32 - 2.4 \times 10^{-9} \text{ cm}^3 \text{ s}^{-1}$. Essentially all of the ions, including the molecular ion and the large fragment ions, undergo decomposition upon collision with neutral molecules after they are kinetically excited to an energy range of 1–5 eV, forming a variety of small hydrocarbon ions. Many of the decomposition product ions in turn are capable of further reacting with *n*-octane. Isotope reagents have been utilized in experiments to probe the type of the ion-molecule reactions studied. © 2001 American Institute of Physics. [DOI: 10.1063/1.1334898]

I. INTRODUCTION

The role played by the charged particle collisions in combustion and ignition has been reevaluated recently.¹ Because ion-molecule reactions are typically 100 times faster than the neutral particle reactions, they are considered to be capable of enhancing the rate of combustion or ignition by breaking chemical bonds, creating radicals, and speeding up the first and slowest step in the combustion reaction. The reactions of selected ions including N_2^+ , O_2^+ , N^+ , O^+ , NO^+ , and H_3O^+ with *n*-octane and iso-octane have been recently studied by Arnold *et al.*^{2,3} While N_2^+ , O_2^+ , N^+ , and O^+ react at collision rates via charge transfer, NO^+ and H_3O^+ react primarily via hydride-abstraction and proton transfer, respectively, with relatively slow rates. The products of these ion-molecule reactions are found to be the types of radicals that would result from a conventional combustion initiation step involving thermal decomposition of alkanes at higher temperature.

In this paper we report on our study using Fourier-transform mass spectrometry on the electron impact ionization and ion chemistries of *n*-octane. The ion chemistries under study are the reactions of the ions from *n*-octane with the parent molecule at pressures of 10^{-7} Torr so that the two-body collision kinetics only are measured. To further estimate the contribution of the ion chemistries to the ignition process, we are probing the possibility of ion recycling in which the reactant ions are regenerated enabling the ionic chain reaction to be continued. Our study finds that only the

small fragment ions react at thermal energy with *n*-octane to form larger ions that mostly are unreactive with *n*-octane. Therefore, one possible way to regenerate the reactive ions is to kinetically excite the larger ions and have them undergo collisions with neutral target molecules yielding small fragment ions. Our preliminary results of this aspect will be discussed. To probe the mechanism of ion-molecule reactions, isotope reagents, *n*- C_8H_{18} and *n*- C_8D_{18} , are used in experiments in which the isotope product distribution and the kinetic isotope effects are measured.

The data presented here provide some basic data for the modeling of spark ignition. The simulation of spark ignition is often separated into two parts: breakdown phase and glow phase. For the breakdown phase, the majority of simulations use a fluid model that is computationally easy but without consideration of the details of the electron and ion kinetics.^{4–7} With the advent of more powerful computers, breakdown simulations using kinetic models that make use of knowledge of the ionization cross sections are becoming more popular.^{8–11} For the glow phase, most of the simulation work involves only the neutral particle reaction scheme.^{12–18} This is probably not adequate because, at the early stages of expansion of the ionized kernel in spark ignition, the concentration of ions relative to the neutral radicals is significant. In recent years, at least two simulation works that use mechanisms involving the ion-molecule reactions have been reported.^{19,20}

II. EXPERIMENT

All experiments are performed on a modified Extrel Fourier-transform mass spectrometer (FTMS) equipped with a cubic ion cyclotron resonance trapping cell (5 cm on a

^{a)} Author to whom correspondence should be addressed. Fax: 937-656-4657; Electronic mail: alan.garscadden@wpafb.af.mil

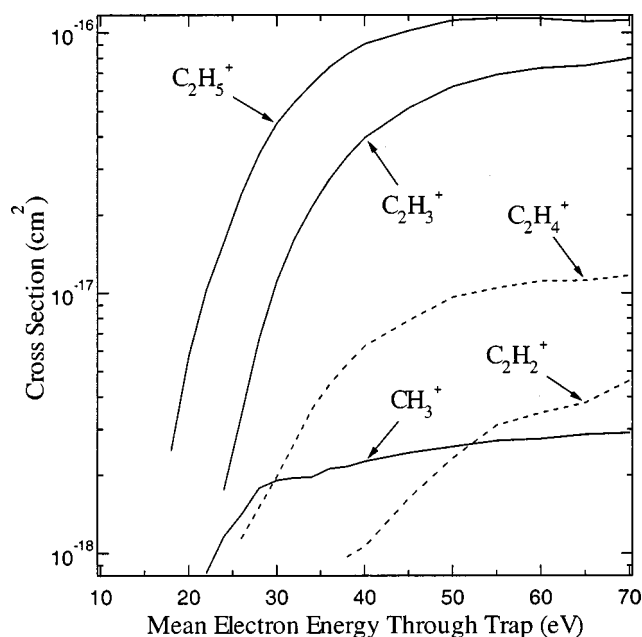


FIG. 1. Cross sections for the formation of C_1^+ and C_2^+ ions from *n*-octane by electron impact.

side) and a 2 T superconducting magnet.²¹ Typically, octane (99+%, Aldrich) is mixed with argon (99.999%, Matheson Research Grade) with a ratio about 1:1 to a total pressure of ~ 2 Torr, as determined by capacitance manometry. For the isotope reagent experiments, octane- d_{18} (98+% atom % D, Aldrich) is mixed with octane and argon with a ratio of $\sim 1:1:2$. The mixture is admitted through a precision leak valve into the FTMS system. Ions are formed by electron impact in the trapping cell at pressures in the 10^{-7} Torr range. An electron gun (Kimball Physics ELG2, Wilton, NH) irradiates the cell with a few hundred picocoulombs of low-energy electrons. The motion of the ions is constrained radially by the superconducting magnetic field and axially by an electrostatic potential (1 V) applied to the trap faces that are perpendicular to the magnetic field. Ions of all mass-to-charge ratios are simultaneously and coherently excited into cyclotron orbits using a stored waveform^{22,23} applied to two opposing trap faces which are parallel to the magnetic field. Following cyclotron excitation, the image currents induced on the two remaining faces of the trap are amplified, digitized and Fourier analyzed to yield a mass spectrum.

The calculation of cross sections from the mass spectrum intensities requires knowledge of the gas densities, the electron beam current, and the number of ions produced. These calibration issues have been described previously.^{21,24} The intensity ratios of the ions from octane to Ar^+ give cross sections relative to those for argon ionization²⁵ since the pressure ratio of Ar to octane is known. As a cross check, and for ion molecule kinetic analyses, the gas pressure is calibrated using a pulsed valve and a spinning rotor friction gauge (MKS Instruments model SRG2, Burlington, MA) with the vacuum chamber sealed off from the pumps. After passage of the electron beam through the ion trap, electron current is collected on a Faraday cup and recorded with a digital oscilloscope. The quantitative relationship between

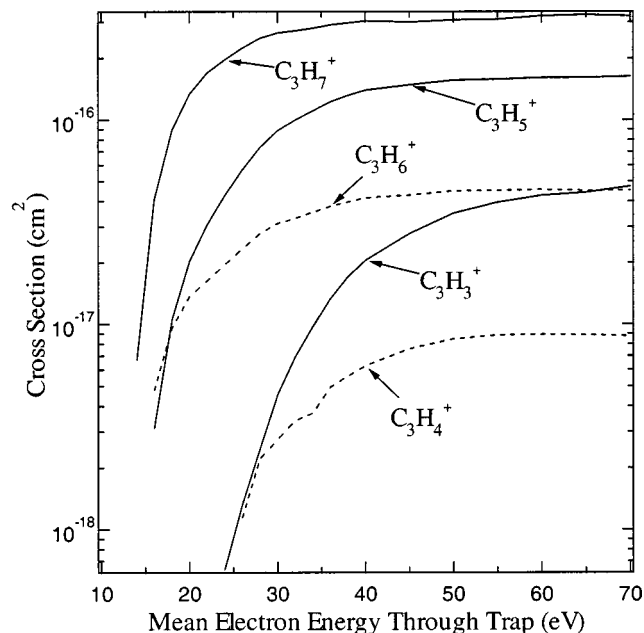


FIG. 2. Cross sections for the formation of C_3^+ ions from *n*-octane by electron impact.

the image current and the number of ions is based on a lengthy, but elementary, solution of Maxwell's equations for the cubic ICR cell. This is required to quantify both excitation of the ions and detection of the resulting image current.²¹

The technique of collision-induced dissociation (CID) in FTMS has been described previously.²⁶ The ion to be studied is first isolated using a stored waveform and then excited by another waveform to a larger orbit, increasing its kinetic energy. By varying the radius of the orbit (typically 0.1–1.0 cm radius), the kinetic energy can be varied from a fraction of an eV to a few hundred eV. This excitation to higher energy typically takes place in a time short compared to the collision time with the neutral background gas. In a subsequent collision with a neutral gas molecule, part of the kinetic energy may be converted to internal energy (which may lead to dissociation) or the ion may simply be cooled by elastic scattering. Because the ion may undergo several collisions before it dissociates, the kinetic energy the ion possesses when dissociation occurs is not well defined. Only the maximum kinetic energy can be specified for CID experiments with the FTMS.

III. RESULTS AND DISCUSSION

Electron impact ionization cross sections of *n*-octane over an energy range of 10–70 eV are shown in Figs. 1–4. As the electron impact energy is increased, the total ionization cross section rises dramatically near threshold (12–20 eV) and levels off at ~ 60 eV with a value of $1.4 \pm 0.2 \times 10^{-15} \text{ cm}^2$. A significant amount of the molecular ion is observed, and fragment ions range from C_1^+ to C_6^+ with the complete absence of C_7^+ . As demonstrated in a previous study by MacColl,²⁷ when the linear hydrocarbon molecules become larger, the amounts of fragment ions M-1 and M-15 become vanishingly smaller, which is a characteristic crack-

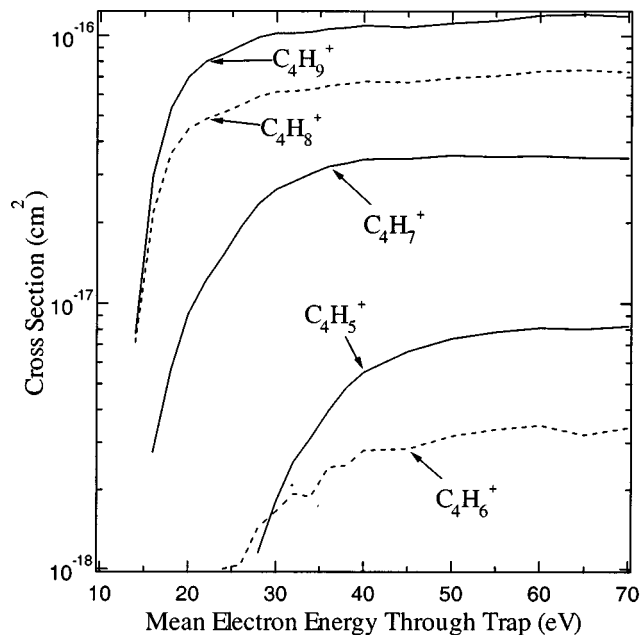
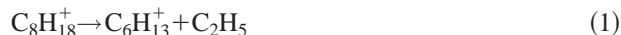


FIG. 3. Cross sections for the formation of C_4^+ ions from *n*-octane by electron impact.

ing pattern for the normal alkanes.²⁸ Table I lists the absolute and relative cross sections of these ions at 20, 50, and 70 eV. At these energies $C_3H_7^+$ is the most abundant ion, and in each group of C_n^+ ions $C_nH_{2n+1}^+$ is always the major ion. These features generally hold true at all energies except for $E \leq 16$ eV where $C_3H_7^+$ is less than $C_6H_{13}^+$ and, for C_{4-6}^+ near their thresholds, $C_nH_{2n}^+$ are slightly more intense than $C_nH_{2n+1}^+$. All of the fragment ions are formed by the fragmentation of the molecular ion via (1) primary decomposition (i.e., decomposition directly from the molecular ion), or

(2) successive decomposition (i.e., subsequent decomposition from the daughter ions). The fragmentation can be (1) a simple C–C bond cleavage, or (2) accompanied by atom rearrangement. The fact that the C_7^+ ion is absent suggests that the formation of $C_6H_{13}^+$ or $C_6H_{12}^+$ from *n*-octane is a primary process,



While reaction (1) is a simple C–C bond split process, reaction (2) is via a H-atom rearrangement before or during the C–C bond cleavage. It should be pointed out that it is possible for the H-atom rearrangement to occur after the C–C bond cleavage in both reactions (1) and (2), yielding a more stable ion isomer(s). It has been generally observed that, compared to the simple single-bond cleavage, the bond cleavage with rearrangement has a relatively small activation energy and frequency factor.²⁹ The data for $C_6H_{12}^+$ and $C_6H_{13}^+$ in Fig. 4 exhibit this characteristic: the $C_6H_{12}^+$ cross section has a lower onset energy but rises relatively slowly, while the $C_6H_{13}^+$ cross section has a higher onset energy but rises faster. The formation of $C_5H_{11}^+$ vs $C_5H_{10}^+$ and $C_4H_9^+$ vs $C_4H_8^+$ near their thresholds exhibit similar trends and the following fragmentation processes at low ionizing energies are implied:



In the literature, two studies using labeled compounds suggested that $C_6H_{13}^+$, $C_5H_{11}^+$, and $C_4H_9^+$ are formed from octane chiefly by primary processes³⁰ and that these primary processes are via a simple C–C bond split.³¹ In summary, we believe that the major neutral fragments produced from the electron impact ionization at low energies (i.e., ≤ 16 eV) are C_2H_5 and C_2H_6 ; in addition, relatively small amounts of C_3H_7 , C_3H_8 , C_4H_9 , and C_4H_{11} are present. As electron energy increases, successive decomposition increases resulting in complex fragmentation paths, which makes deducing the neutral fragments more difficult.

Among the ions generated from the electron impact ionization of *n*-octane, only $C_4H_7^+$ and smaller ions undergo gas-phase reactions with *n*-octane molecule under the condition of 10^{-7} Torr gas pressures. The reaction kinetics for some selected reactive ions with ionization cross sections greater than 10^{-17} cm² at 50 eV are studied and the results are shown in Table II. The reactant ions are not thermalized prior to the reactions and therefore may have higher internal energies, which have effect on the reaction kinetics as discussed later. As *n* in C_n^+ gets smaller, the reaction rate increases and a greater variety of product ions is generated. The major product ions are $C_5H_{11}^+$ and $C_4H_9^+$. Relatively small amounts of $C_3H_7^+$ and $C_3H_5^+$ are also produced from small C_n^+ , and these two product ions can undergo secondary reactions with *n*-octane to finally form $C_5H_{11}^+$ and $C_4H_9^+$ that are unreactive with *n*-octane. The reactions in Table II

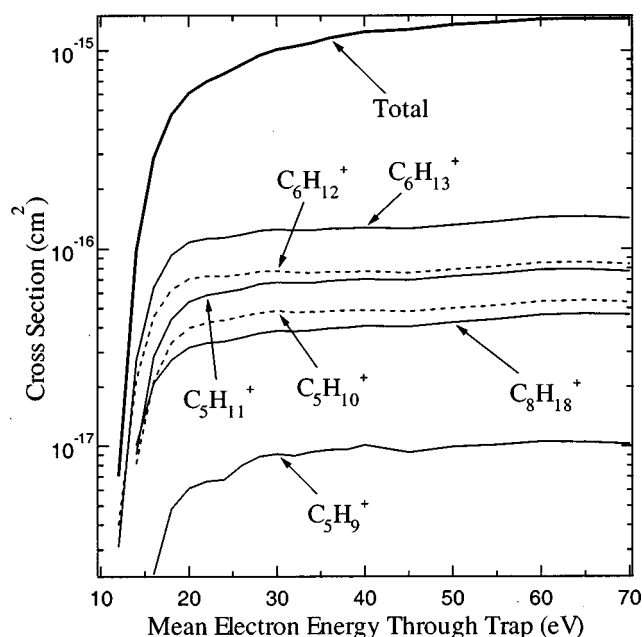


FIG. 4. Cross sections for the formation of C_5^+ , C_6^+ , and C_8^+ ions from *n*-octane by electron impact. Also shown are the total ionization cross sections.

TABLE I. Cross sections ($\sigma, 10^{-16} \text{ cm}^2$) and relative intensities of the ions from *n*-octane at 20, 50, and 70 eV electron impact. Ions are listed in the order of (a) increasing mass, and (b) decreasing cross section for the purpose of mass spectrometry references at 70 eV.

| (a) | 20 eV | | 50 eV | | (b) | 70 eV | |
|-----------------------------|----------|-----------|----------|-----------|-----------------------------|----------|-----------|
| | σ | Rel. int. | σ | Rel. int. | | σ | Rel. int. |
| CH_3^+ | 0.005 | 0.4 | 0.026 | 1 | C_3H_7^+ | 3.2 | 100 |
| C_2H_2^+ | — | — | 0.023 | 1 | C_3H_5^+ | 1.6 | 51 |
| C_2H_3^+ | — | — | 0.62 | 20 | $\text{C}_6\text{H}_{13}^+$ | 1.4 | 44 |
| C_2H_4^+ | — | — | 0.096 | 3 | C_4H_9^+ | 1.2 | 37 |
| C_2H_5^+ | 0.057 | 4 | 1.1 | 36 | C_2H_5^+ | 1.1 | 35 |
| C_3H_3^+ | — | — | 0.35 | 11 | $\text{C}_6\text{H}_{12}^+$ | 0.84 | 26 |
| C_3H_4^+ | — | — | 0.085 | 3 | C_2H_3^+ | 0.80 | 25 |
| C_3H_5^+ | 0.20 | 15 | 1.6 | 51 | $\text{C}_5\text{H}_{11}^+$ | 0.77 | 24 |
| C_3H_6^+ | 0.14 | 10 | 0.45 | 15 | C_4H_8^+ | 0.73 | 23 |
| C_3H_7^+ | 1.3 | 100 | 3.1 | 100 | $\text{C}_5\text{H}_{10}^+$ | 0.54 | 17 |
| C_4H_5^+ | — | — | 0.074 | 2 | C_3H_3^+ | 0.47 | 14 |
| C_4H_6^+ | — | — | 0.031 | 1 | $\text{C}_8\text{H}_{18}^+$ | 0.46 | 14 |
| C_4H_7^+ | 0.091 | 7 | 0.36 | 12 | C_3H_6^+ | 0.45 | 14 |
| C_4H_8^+ | 0.45 | 33 | 0.69 | 23 | C_4H_7^+ | 0.35 | 11 |
| C_4H_9^+ | 0.70 | 52 | 1.1 | 36 | C_2H_4^+ | 0.12 | 4 |
| C_5H_9^+ | 0.061 | 5 | 0.10 | 3 | C_5H_9^+ | 0.10 | 3 |
| $\text{C}_5\text{H}_{10}^+$ | 0.40 | 30 | 0.50 | 16 | C_3H_4^+ | 0.088 | 3 |
| $\text{C}_5\text{H}_{11}^+$ | 0.54 | 40 | 0.73 | 24 | C_4H_5^+ | 0.082 | 3 |
| $\text{C}_6\text{H}_{12}^+$ | 0.71 | 53 | 0.78 | 26 | C_2H_2^+ | 0.046 | 1 |
| $\text{C}_6\text{H}_{13}^+$ | 1.1 | 81 | 1.3 | 43 | C_4H_6^+ | 0.034 | 1 |
| $\text{C}_8\text{H}_{18}^+$ | 0.32 | 24 | 0.42 | 14 | CH_3^+ | 0.029 | 1 |

proceed through one or more of the following mechanisms that have been proposed in the literature for ion-molecule reactions involving paraffin molecules: oxidative-insertion-complex formation, charge-transfer, $\text{H}^{+,0,-}$ -abstraction, or

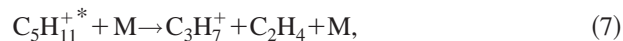
TABLE II. Rate coefficients and branching ratios of gas-phase reactions of some selected C_nH_m^+ with *n*-octane. Reactant ions are generated from 50 eV electron impact ionization and have not been thermalized prior to the reactions.

| Reactant ion | Rate ($10^{-9} \text{ cm}^3 \text{ s}^{-1}$) | Product ion | Branching ratio % |
|--------------------------|------------------------------------------------|-----------------------------|-------------------|
| C_2H_3^+ | 2.4 | $\text{C}_5\text{H}_{11}^+$ | 35 |
| | | C_4H_9^+ | 44 |
| | | C_3H_7^+ | 15 |
| | | C_3H_5^+ | 6 |
| C_2H_5^+ | 1.7 | $\text{C}_5\text{H}_{11}^+$ | 40 |
| | | C_4H_9^+ | 44 |
| | | C_3H_7^+ | 13 |
| | | C_3H_5^+ | 3 |
| C_3H_3^+ | 0.74 | $\text{C}_5\text{H}_{11}^+$ | 49 |
| | | C_4H_9^+ | 46 |
| | | C_3H_7^+ | 5 |
| C_3H_5^+ | 1.1 | $\text{C}_5\text{H}_{11}^+$ | 46 |
| | | C_4H_9^+ | 44 |
| | | C_3H_7^+ | 10 |
| C_3H_6^+ | 1.5 | $\text{C}_5\text{H}_{11}^+$ | 44 |
| | | C_4H_9^+ | 42 |
| | | C_3H_7^+ | 14 |
| C_3H_7^+ | 0.69 | $\text{C}_5\text{H}_{11}^+$ | 59 |
| | | C_4H_9^+ | 41 |
| C_4H_7^+ | 0.32 | $\text{C}_5\text{H}_{11}^+$ | 54 |
| | | C_4H_9^+ | 46 |

alkide (R^-)-abstraction. To probe the reaction mechanisms, different ions from *n*-octane are isolated and allowed to react individually with *n*- C_8H_{18} and, in another separate experiment, with a mixture of *n*- C_8H_{18} and *n*- C_8D_{18} (1:1 ratio). No isotope exchange between the reactant ion and *n*-octane has been observed for all of the reactions in Table II. For example, when C_3H_7^+ reacts with $[\text{C}_8\text{H}_{18}, \text{C}_8\text{D}_{18}]$, only $\text{C}_5\text{H}_{11}^+$, $\text{C}_5\text{D}_{11}^+$, C_4H_9^+ , and C_4D_9^+ are detected. No mixed-isotope ions, such as $\text{C}_5\text{HD}_{10}^+$ or C_4HD_8^+ , are present. This finding appears to exclude the possibility of an oxidative-insertion-complex formation mechanism and a $\text{H}^{+,0,-}$ -abstraction mechanism; with these mechanisms the isotope in the reactant ions should have been more or less retained in the product ions. A charge-transfer mechanism is also unlikely based on the fact that many reactant ions have lower ionization potentials than the appearance potentials of the product ions by a few eV, which means that the reactions in Table II would have been rather endothermic if they were via the charge-transfer mechanism. For example, C_2H_5^+ reacting with *n*-octane via charge-transfer to produce $\text{C}_5\text{H}_{11}^+$ and C_4H_9^+ would be endothermic by 3.0 and 2.8 eV, respectively.³² Therefore, only the hydride- and alkide-abstractions are left as candidates for the possible reaction mechanisms. Some decades ago two studies of the chemical ionization on C_6 and C_{10} paraffins using CH_4 , respectively, found the M-1 ion (M represents molecular mass) to be the most abundant ion from the ion-molecule reactions.^{33,34} It was suggested that C_2H_5^+ generated from CH_4 acted as a H^- abstractor to produce the M-1 ion from C_6 or C_{10} molecules, and the M-1 ion underwent further decomposition to form smaller fragment ions. In another study in the 1970s Lias *et al.*³⁵ demonstrated that C_2H_5^+ and C_3H_7^+ react with

n-alkanes, including *n*-octane, exclusively via hydride transfer to produce M-1 ions. The reaction rate of $C_3H_7^+$ reported in that study, roughly equal to the collision rate, is about twice as large as what we observed. The differences between the experimental results from the studies mentioned above and ours in Table II may be due to different energy content in the reactant ions. One may argue that because in our experiments $C_3H_7^+$ is hot, it may react with *n*- C_8H_{18} via hydride-transfer followed by dissociation to produce partially $C_3H_7^+$ itself, making the apparent reaction rate smaller. In the isotope reagent experiments mentioned earlier, we do not find $C_3D_7^+$ to be produced from the reaction of $C_3H_7^+$ with *n*- C_8D_{18} , which excludes the above argument to be the explanation of our reaction rate of $C_3H_7^+$ differing from Lias *et al.*'s. In our experiments, no M-1 ion from any of the ion-molecule reactions studied has been found. Also, we observed no significant kinetic isotope effect in the isotope reagent experiments. For example, $C_3H_7^+$ reacting with [C_8H_{18}, C_8D_{18}] produces equal amounts of $C_5H_{11}^+$ vs $C_5D_{11}^+$, and equal amounts of $C_4H_9^+$ vs $C_4D_9^+$; also, when $C_3D_7^+$ is used as the reactant ion, the reaction rate and the product distribution remain the same as those for $C_3H_7^+$. We propose that the alkyl-transfer is likely to be involved in the majority of the reactions listed in Table II. However, an alternate mechanism by hydride-transfer followed by dissociation is also possible, although our experiments do not show a kinetic isotope effect which would support hydride-transfer mechanism.

The chemistries of ions with increased kinetic energy have also been studied. Each of the different ions is isolated and then kinetically excited to a certain energy level before there is time to react with *n*-octane. While a thorough examination on collision-induced dissociation (CID) of the *n*-octane ions in the kinetic energy range up to 500 eV is underway, we report here only the CID results at relatively low energies, ~ 1 –5 eV laboratory frame, as these energies are on the order of the upper limit of the kinetic energies of ions in the spark ignition process. Considering that the reactant ions are not initially thermalized as discussed earlier, we expect the energy level of the ions after excitation should be higher than calculated based on the excitation waveform, but not likely to be more than a few eV. The CID results from FTMS experiments are usually presented qualitatively or semi-quantitatively, because with today's FTMS techniques reliable CID reaction rates at well-defined energies are difficult to acquire even for reactant ions that are initially thermalized. Here we report only the products from the kinetically excited ion reactions. At these elevated energies ions can potentially undergo all of the possible reactions including charge-transfer and H^- or R^- abstraction, as well as CID. We find that essentially only the CID processes are involved. For example, when $C_5H_{11}^+$ is kinetically excited (here designated as $C_5H_{11}^{+*}$) we find,

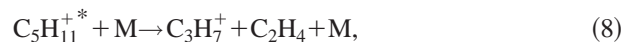


where M represents the neutral collision target. The neutral fragment, C_2H_4 , in the above equation only represents the authors' estimate, considering that the ion has only a few eV

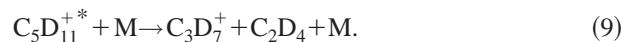
TABLE III. Products and the isotope effects of the collision-induced dissociation of the kinetically excited ions. The neutral fragment products represent only the authors' proposed scheme. The kinetic isotope effects presented here are the ratios of the reaction rates of the *h*-isotope and *d*-isotope reactant ions (k_H/k_D).

| Reactant ions | Products | Kinetic isotope effect |
|------------------|------------------------|------------------------|
| $C_8H_{18}^{+*}$ | $C_6H_{13}^+ + C_2H_5$ | 0.7 |
| | $C_6H_{12}^+ + C_2H_6$ | 0.8 |
| | $C_5H_{11}^+ + C_3H_7$ | — |
| | $C_4H_9^+ + C_4H_9$ | — |
| | $C_3H_7^+ + C_5H_{11}$ | — |
| $C_6H_{13}^{+*}$ | $C_4H_9^+ + C_2H_4$ | 1.0 |
| | $C_3H_7^+ + C_3H_6$ | 1.3 |
| $C_6H_{12}^{+*}$ | $C_5H_9^+ + CH_3$ | 1.0 |
| | $C_4H_8^+ + C_2H_4$ | 0.6 |
| | $C_4H_7^+ + C_2H_5$ | 0.6 |
| | $C_3H_6^+ + C_3H_6$ | 0.7 |
| | $C_3H_5^+ + C_3H_7$ | 0.6 |
| $C_5H_{11}^{+*}$ | $C_3H_7^+ + C_2H_4$ | 1.0 |
| $C_5H_{10}^{+*}$ | $C_4H_7^+ + CH_4$ | 0.8 |
| | $C_3H_6^+ + C_2H_4$ | 1.0 |
| $C_4H_9^{+*}$ | $C_3H_5^+ + CH_4$ | 0.8 |
| | $C_2H_3^+ + C_2H_4$ | 0.9 |
| $C_4H_8^{+*}$ | $C_3H_5^+ + CH_4$ | 0.8 |
| $C_3H_7^{+*}$ | $C_3H_5^+ + H_2$ | 0.6 |
| $C_3H_6^{+*}$ | $C_3H_5^+ + H$ | 0.2 |

energy, and that increased fragmentation requires more energy. The CID process is distinguished from the other endothermic reactions by the product isotope pattern. When $C_5H_{11}^+$ reacts with a 1:1 mixture of C_8H_{18} and C_8D_{18} , only $C_3H_7^+$ is observed:



where $M = [C_8H_{18}, C_8D_{18}]$. The amount of product $C_3D_7^+$ is insignificant. To determine if this product selectivity is not due to the kinetic isotope effect, $C_5D_{11}^+$ is used as the reactant ion. Then, essentially only $C_3D_7^+$ is observed:

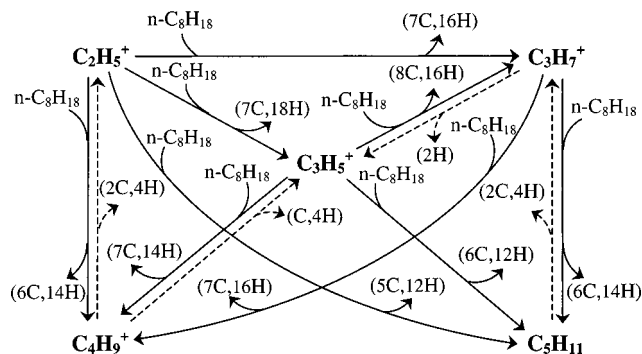


Clearly, these experimental results indicate that the reaction of $C_5D_{11}^{+*}$ is a CID process. Similar experiments show that CID is also the major endothermic reaction observed for other kinetically excited ions, with the results shown in Table III. For the molecular ion $C_8H_{18}^{+*}$, the reaction with [C_8H_{18}, C_8D_{18}] produces $C_5H_{11}^+$, $C_4H_9^+$, $C_3H_7^+$, and relatively small amounts of the corresponding *d*-isotope ions, which suggests that the CID of $C_8H_{18}^{+*}$ is mixed with other reaction(s). This other reaction is unlikely to be a H^- or R^- abstraction reaction because all of the C atoms in this $C_8H_{18}^+$ are fully ligated. The charge transfer reaction is most likely the one involved. In Table III, the kinetic isotope effects are also listed. We provide the ratios of the reaction rates of the *h*-isotope and *d*-isotope reactant ions (k_H/k_D). While the isotope effects for most of the reactions in Table III are not remarkable, the inverse isotope effect for reaction $C_3H_6^{+*} \rightarrow C_3H_5^+ + H$ is significant and is not consistent with its

seemingly simple C–H bond cleavage process. Thus whether this reaction is in fact purely a collision-induced dissociation is not clear at this point.

The CID product ions, if smaller than C_4H_7^+ , are observed to undergo the same reactions listed in Table II for the corresponding ions from the electron impact ionization, although whether the CID product ions have the same structures as the corresponding ions from the electron impact ionization is in question. A study in the 1970s on CID of isomeric octane ions demonstrated that structurally isomeric ions isomerize to a common structure prior to decomposition.³⁶ On the other hand, another study showed that the alkyl ions from the electron impact ionization on hydrocarbons might be a mixture of structural isomers.³⁷ We do not see different reaction rates for the isomers, when there are any, for all of the reactions in Table II, i.e., no biexponential decay of the reactant ion has been observed.

From the results presented above we conclude that, if the ion temperature is high enough to drive its “thermal decomposition,” there are many reaction cycles in the *n*-octane plasma: the reactant ion is reacted away with *n*-octane, while the product ion decomposes to regenerate the reactant ion, and the reaction goes on. Some important cycles are shown in scheme 1.



In the scheme, the dash lines denote the endothermic reaction paths (CIDs, the neutral collision target not shown), and the neutral products are shown in parentheses only for the purpose to make the mass balance. Such a reaction cycle each time converts *n*-octane to other smaller species, such as C₇H₄, CH₄, or H₂.

IV. SUMMARY

Electron impact ionization on *n*-octane produces molecular ions and fragment ions that range from C_1^+ to C_6^+ , with a total ionization cross section of $1.4 \pm 0.2 \times 10^{-15} \text{ cm}^2$ between 60 and 70 eV. At low energies ($\leq 16 \text{ eV}$) $C_6H_{13}^+$ and $C_6H_{12}^+$ are the most abundant ions and C_2H_5 and C_2H_6 are believed to be the major neutral fragments. As the electron energy increases, $C_3H_7^+$ becomes the most abundant ion and the neutral fragments become more difficult to deduce. Among the ions generated from electron impact ionization on *n*-octane, only $C_4H_7^+$ and smaller ions can react with the parent molecule, mainly producing $C_5H_{11}^+$ and $C_4H_9^+$, probably via an alkyl-abstraction mechanism. The reaction rates vary from 0.32 to $2.4 \times 10^{-9} \text{ cm}^3 \text{ s}^{-1}$, with a general trend of increasing reactivity with the decreasing number of carbon

atoms in the reactant ion. Upon being kinetically excited to $\sim 1\text{--}5$ eV, most of the ions studied undergo decomposition forming smaller ions which can react again with *n*-octane, and the reaction cycle continues.

Usually one may expect that after the electron impact ionization, the relaxation of the ion composition by ion-molecule reactions leads to a stable ion composition; the ion-molecule reactions convert the reactive ions to more stable product ions and at the end all of the ions are unreactive. The present study demonstrates that a slightly elevated energies the *reactive* ions can be recycled, and reaction chains can be accomplished that repeatedly convert large paraffins into smaller hydrocarbon molecules. In certain aspects this process resembles the neutral radical chain reaction in combustion or ignition. Ion reactions are in general much faster than the neutral particle reactions and, therefore, they should play more important roles at the early ignition stages until the high concentration of neutral radicals builds up and the thermal cracking dominates the combustion mechanisms. High-energy ions are realistic at the very early stage of spark ignition; the temperature in the spark kernel can be well above 10 000 K,^{18,38} although the discharge volume at this stage is small and the gas rapidly relaxes to temperatures of a few thousand K within microseconds. Furthermore, it might be possible to design an ignition device that can increase the kinetic energy of the ions and thus enhance the overall efficiency of the ignition.

ACKNOWLEDGMENT

The authors thank the Air Force Office of Scientific Research for support.

- ¹S. Williams, A. J. Midey, S. T. Arnold, P. M. Bench, A. A. Viggiano, R. A. Morris, L. Q. Maurice, and C. D. Carter, "Progress on the investigation of the effects of ionization on hydrocarbon/air combustion chemistry," AIAA Paper No. 99-4907.
- ²S. T. Arnold, A. A. Viggiano, and R. A. Morris, *J. Phys. Chem. A* **101**, 9351 (1997).
- ³S. T. Arnold, A. A. Viggiano, and R. A. Morris, *J. Phys. Chem. A* **102**, 8881 (1998).
- ⁴R. Morrow, *Phys. Rev. A* **32**, 1799 (1985).
- ⁵S. Dhali and P. F. Williams, *Phys. Rev. A* **31**, 1219 (1985).
- ⁶P. Bayle and B. Cornebois, *Phys. Rev. A* **31**, 1046 (1985).
- ⁷C. Wu and E. E. Kunhardt, *Phys. Rev. A* **37**, 4396 (1988).
- ⁸L. E. Kline and J. G. Stambis, *Phys. Rev. A* **5**, 794 (1972).
- ⁹J. M. Geary and G. W. Penney, *Phys. Rev. A* **17**, 1483 (1978).
- ¹⁰A. E. Rodriguez, W. L. Morgan, K. J. Touryan, W. M. Money, and T. H. Martin, *J. Appl. Phys.* **70**, 2015 (1991).
- ¹¹E. E. Kunhardt and Y. Tzeng, in *Proceedings of the IV International Symposium on Gaseous Dielectrics*, edited by L. G. Christophorou (Plenum, New York, 1984), p. 146.
- ¹²D. Bradley and F. K-K. Lung, *Combust. Flame* **69**, 71 (1987).
- ¹³G. T. Kalghargi, *Combust. Flame* **77**, 321 (1989).
- ¹⁴Y. Ko, V. S. Arpaci, and R. W. Anderson, *Combust. Flame* **83**, 74 (1991).
- ¹⁵Y. Ko, R. W. Anderson, and V. S. Arpaci, *Combust. Flame* **83**, 105 (1991).
- ¹⁶K. Ishii, T. Tsukamoto, Y. Ujiie, and M. Kono, *Combust. Flame* **91**, 153 (1992).
- ¹⁷C. G. Foatche, T. G. Kreutz, and C. K. Law, Joint Technical Meeting of the Central States, Western States, and Mexican National Sections of the Combustion Institute, April 23–26, 1995, San Antonio, TX.
- ¹⁸M. Schafer, R. Schmidt, and J. Kohler, Twenty-Sixth Symposium (International) on Combustion/The Combustion Institute, 1996, pp. 2701–2708.
- ¹⁹Chul Park, *J. Thermophysics* **3**, 233 (1989).

- ²⁰T. Kravchik and E. Sher, *Combust. Flame* **99**, 635 (1994).
- ²¹K. Riehl, "Collisional detachment of negative ions using FTMS," Ph.D. thesis, Air Force Institute of Technology, Dayton, OH, 1992.
- ²²A. G. Marshall, T. L. Wang, and T. L. Ricca, *J. Am. Chem. Soc.* **107**, 7893 (1985).
- ²³S. Guan, *J. Chem. Phys.* **91**, 775 (1989).
- ²⁴P. D. Haaland, *Chem. Phys. Lett.* **170**, 146 (1990).
- ²⁵R. C. Wetzel, F. A. Baiocchi, T. R. Hayes, and R. S. Freund, *Phys. Rev. A* **35**, 559 (1987).
- ²⁶B. S. Freiser, *Techniques for the Study of Ion Molecule Reactions*, edited by J. M. Farrar and W. H. Saunderson, Jr. (Wiley, New York, 1988), Vol. 20, Chap. 2.
- ²⁷Allan MacColl, *Org. Mass Spectrom.* **17**, 1 (1982).
- ²⁸R. I. Reed, *Ion Production by Electron Impact* (Academic, London, 1962).
- ²⁹D. H. Williams and I. Howe, *Principles of Organic Mass Spectrometry* (McGraw-Hill, London, 1972).
- ³⁰S. Meyerson, *J. Chem. Phys.* **42**, 2181 (1965).
- ³¹K. Levens, H. Heimbach, G. J. Shaw, and G. W. A. Milne, *Org. Mass Spectrom.* **12**, 663 (1977).
- ³²H. M. Rosenstock, K. Draxl, B. W. Steiner, and J. T. Herron, "Energetics of Gaseous Ions," *J. Phys. Chem. Ref. Data* **6**, (1977).
- ³³R. P. Clow and J. H. Futrell, *J. Am. Chem. Soc.* **94**, 3748 (1972).
- ³⁴D. F. Hunt and C. N. McEwen, *Org. Mass Spectrom.* **7**, 441 (1973).
- ³⁵S. G. Lias, J. R. Eyler, and P. Ausloos, *Int. J. Mass Spectrom. Ion Phys.* **19**, 219 (1976).
- ³⁶K. Levens, *Org. Mass Spectrom.* **10**, 43 (1975).
- ³⁷M. L. Gross, *J. Am. Chem. Soc.* **93**, 253 (1971).
- ³⁸E. Sher, J. Ben-Ya'ish, and T. Kravchik, *Combust. Flame* **89**, 186 (1992).